Keratinocyte dynamics modulate the spatial organization of redox signaling during sensory neuron regeneration

Alexandra M. Fister[1, 2, §], Adam Horn[1, §], and Anna Huttenlocher[1, 3, *]

[1]Department of Medical Microbiology and Immunology, University of Wisconsin-Madison, Madison, United States.

[2]Cellular and Molecular Biology Graduate Program, University of Wisconsin-Madison, Madison, United States.

[3]Department of Pediatrics, University of Wisconsin-Madison, Madison, United States.

[§]These authors contributed equally.

[*]Corresponding Author: huttenlocher@wisc.edu

Summary

Epithelial damage leads to early reactive oxygen species (ROS) signaling that regulates sensory neuron regeneration and tissue repair. How the initial type of tissue injury influences early damage signaling and regenerative growth of sensory neurons remains unclear. Previously we reported that thermal injury triggers distinct early tissue responses in larval zebrafish. Here, we found that thermal but not mechanical injury impairs sensory neuron regeneration and function. Real-time imaging revealed an immediate tissue response to thermal injury characterized by the rapid movement of keratinocytes, which was associated with tissue-scale ROS production and sustained sensory neuron damage. Osmotic regulation induced by isotonic treatment was sufficient to limit keratinocyte movement, spatially-restrict ROS production and rescue sensory neuron function. These results suggest that early keratinocyte dynamics regulate the spatial and temporal pattern of long-term signaling in the wound microenvironment during sensory neuron regeneration and tissue repair.

Introduction

Restoration of tissue function following epithelial injury requires the regeneration and activity of peripheral sensory neurons, which innervate the skin[1–3]. In response to tissue damage, sensory neurons undergo rapid and localized axonal degeneration[4,5]. The process of neuronal regeneration first requires the clearance of axon fragments by phagocytes followed by new axonal growth[6]. While peripheral sensory neurons maintain a cell-intrinsic ability to regenerate following injury[7–9], local environmental cues also regulate the response of sensory neurons to tissue damage *in vivo*. Recent advances have identified the contribution of supporting cell populations, paracrine biochemical signaling, and biophysical interactions during sensory neuron regeneration[10–12]. Despite these advances, we have limited understanding of how early signaling in the wound microenvironment is organized and regulates long-term sensory neuron regeneration and tissue repair.

Epidermal keratinocytes are a primary constituent of epithelial tissue and play a critical role in wound healing. In addition to mediating wound closure by actively migrating toward the site of injury, keratinocytes also generate pro-reparative signals such as reactive oxygen species (ROS), which coordinate longer-term repair pathways [13–19]. While transient and localized ROS production promote regeneration and sensory neuron regrowth, chronically elevated ROS are associated with neurodegeneration and disease[17,20,21]. Thus, precise temporal and spatial organization of tissue redox signaling is likely critical for efficient sensory neuron regeneration and tissue repair.

While epithelial tissue is well-adapted to repair from mechanical damage, burn wounds heal poorly. Thermal injury results in chronic pain and lack of sensation, suggesting that an abnormal sensory neuron response contributes to burn wound pathophysiology [22–26]. Despite this, we lack an understanding of why sensory neuron function is impaired after burns. Our previous work has demonstrated persistent inflammation and a loss of an organized collagen matrix that impairs healing after thermal injury in larval zebrafish[27–29].

These features recapitulate human burns and provide a simplified *in vivo* model system to study the regeneration of sensory neurons in the wound microenvironment.

Using real time imaging, we took advantage of the optical transparency of larval zebrafish to dissect dynamic cell-cell interactions in the wound microenvironment following injury. We found that localized thermal injury induced substantial axonal damage and impaired sensory neuron regeneration in the tail fin. Live imaging showed that keratinocytes exhibit rapid collective movement following burns that physically displace sensory neurons. This early keratinocyte movement contributes to elevated ROS at the tissue-scale. Limiting keratinocyte movement through osmotic manipulation spatially restricted ROS production and rescued sensory neuron regeneration and function. Additionally, the antioxidant N-acetyl-cysteine (NAC) improved sensory neuron regeneration, highlighting the need for balanced ROS production to optimize tissue repair. Collectively, our results demonstrate the importance of regulated keratinocyte behavior for early temporal and spatial signal control that leads to long term sensory neuron regeneration and tissue repair.

Results

Peripheral sensory neurons have impaired regeneration after burn injury

To visualize sensory neurons responding to tissue injury, we used 3 days post-fertilization (dpf) *Tg(Ngn1:GFP-Caax)* larval zebrafish that express GFP in sensory neurons[30–32]. Larvae were either mechanically injured by tailfin transection or burn as previously described (**Fig. 1A**)[27]. Intravital imaging of larvae beginning at 24 hours post wound revealed an abnormal axonal morphology in burned larvae compared to mechanical transection, with axons showing fewer branch points (**Fig. 1B**). To evaluate sensory neuron regeneration following injury, we assessed axon density in the wounded tissue. Following transection, axon density was 89.5 ± 0.02% of the density observed in age-matched uninjured larvae 24 hours post wound (hpw). In contrast, we found that burned larvae had significantly impaired sensory axon regeneration, with an axon density of 63.7 ± 0.02% compared to uninjured fins (**Fig. 1C**). This relative decrease was sustained even 96

hours post burn (hpb) with an axon density of only 65.1 ± 0.04% compared to control (**Fig. 1C**). To test whether this regenerative defect was associated with a defect in sensory neuron function, we assessed the touch responsiveness of wounded tissue. Light pressure was applied by an eyelash brush directly to the wound area, and sensory neuron function was scored by the presence of a tail flick reflex[33]. As expected, larvae wounded by transection had a nearly 100% response rate 24 hpw, highlighting the rapid recovery of sensory neurons following mechanical injury (**Fig. 1D**). In contrast, none of the burned larvae were sensitive to touch 24 hpb with partial resolution by 96 hpb (**Fig. 1D**). Importantly, all tested larvae exhibited a tail flick reflex when pressure was applied to the trunk, demonstrating that impaired sensation was limited to the damaged tissue.

We next sought to investigate why sensory neuron function was impaired in burned tissue. For this, we assessed wound-induced axonal damage using zebrafish that express the calcium probe GCaMP. While calcium increase following axonal damage is required for immediate membrane repair and subsequent regeneration, chronically elevated cytosolic calcium is associated with cell death and degeneration[34]. Therefore, imaging of neuronal calcium flux enables real-time labeling of neuronal damage in larval zebrafish[35]. Using *Tg(Elavl3:GCaMP5)* larvae, we observed minimal calcium flux under homeostatic conditions. However, the neurotoxin sodium azide elicited widespread and long-lasting calcium-positive punctae, indicating neuronal damage (**Fig. S1A**)[35]. Unlike Ngn1, the Elavl3 promoter is expressed by both sensory and motor neurons. To ensure that the calcium increase in epithelial tissue was specific to sensory neurons, we depleted sensory neurons by injecting Ngn1 morpholino into Elavl3:GCaMP5-expressing embryos. As expected, no calcium increase was detected in Ngn1 depleted larvae following injury (**Fig. S1B**).

In agreement with previous observations of axonal damage following mechanical injury[6,20,36], tailfin transection resulted in spatially localized axonal damage that was almost completely resolved by 1 hpw (**Fig. 1E**). In contrast, burn injury resulted in a distinct temporal and spatial profile of sensory axon damage. While initial wound-induced sensory neuron calcium signal appeared to be localized to burned tissue, axonal damage continued to spread across the tissue for approximately 6 hours (**Fig. 1E**). This raised the question of whether

axonal damage was restricted to epithelial tissue directly impacted by injury, as observed in transected larvae. To label wounded epithelium, we used the lipophilic dye FM 1-43, which is commonly used to label damaged cells[37]. Immediately following either transection or thermal injury, axonal damage overlapped spatially with wounded epithelial tissue (**Fig. 1F, G**). However, by 6 hpb, there was widespread damage to axons that extended beyond the initial wound area (**Fig. 1F, G**). These findings suggest that burn injury induces axonal damage that accumulates over time and is spatially uncoupled from the surrounding epithelial damage.

The burn wound microenvironment contributes to impaired sensory neuron regeneration

To determine if early wound signaling regulates sensory neuron regeneration, we used a two-wound model to excise the burned tissue. In this system, zebrafish were first injured by either tailfin transection or burn and then a second transection injury was carried out either 5 minutes post-wound to allow for immediate signaling, or 6 hours post wound to coincide with the timing of peak axonal damage. The secondary transection was performed so that all of the burned tissue was excised (**Fig. 2A, B**). As expected, larvae that underwent initial transection showed complete restoration of sensory function by 24 hpw, regardless of the timing of the secondary transection injury, highlighting the ability of zebrafish to efficiently heal from mechanical damage (**Fig. 2C-E**). In burned larvae, early transection after thermal injury restored axonal regeneration and sensory function similar to transected tailfins when measured 24 hours after the second wound, suggesting that burn injury does not immediately affect sensory neurons differently than mechanical damage. However, when burned tissue was excised after 6 hours, we noted significant defects in both axonal regeneration and sensory function compared to larvae that received two transection injuries (**Fig. 2C-E**). These findings suggest that the local wound environment impairs sensory neuron regeneration following burn injury.

Burn injury induces coordinated keratinocyte and sensory neuron movement

To understand how burn injury triggers a damaging wound microenvironment, we live imaged the behavior of keratinocytes and sensory neurons after burn. Imaging revealed the close association between epithelial cells and sensory neurons, in accordance with the innervation of the epidermis by the sensory neurons

(**Fig. 3A-C**) [20,38,39]. Live-imaging of *Tg(Krt4:Utrophin-GFP)* larvae that express the actin probe Utrophin under a pan-keratinocyte promoter allowed for visualization of keratinocyte dynamics following either mechanical or burn injury. In response to transection, we initially observed characteristic epithelial cell contraction at the wound edge; however, keratinocytes distal to the wound edge remained relatively stationary (**Fig 3D; Supplemental Movie 1**). In contrast, burn wounding resulted in a rapid collective movement of keratinocytes toward the site of tissue damage (**Fig 3D; Supplemental Movie 1**). At times, the keratinocytes exhibited chaotic movement and appeared to lose contact with their neighbors. To quantify the rapid movement of keratinocytes in burn injured larvae, we used *Tg(Krtt1c19e:acGFP)* zebrafish to specifically label motile basal epithelial cells (**Fig. S2A**) [40–42]. Live-imaging experiments revealed that basal keratinocytes, on average, move a total distance of 205.7±10.7 μm in the first hour following burn injury, which was significantly greater than the 58.9±5.8 μm of migration observed following tailfin transection (**Fig 3E; Fig. S2A, B**).

The axons of sensory neurons are ensheathed within actin-rich channels running through basal keratinocytes (**Fig. 3C**) [43,44]. Given the chaotic and sustained keratinocyte movement associated with burn injury, next we tested if dysregulated keratinocyte movement resulted in increased sensory neuron damage as neurons and epithelial cells slide against one another. Simultaneous imaging of keratinocytes and sensory neurons following thermal injury revealed that sensory neuron movement is coordinated with the keratinocytes (**Fig 3F; Supplemental Movie 2**). However, it remained unclear whether neurons were being damaged as the cells moved. To assess the timing of axonal damage, we performed live-imaging following burn injury using *Tg(Elavl3:GCaMP5)* larvae. While initial burn-induced axonal damage was apparent, we observed no additional damage, reported by calcium flux, during keratinocyte movement (**Fig. 3G; Supplemental Movie 3**). These findings suggest that the initial keratinocyte movement may not directly result in sensory neuron damage.

Keratinocyte movement induced by thermal injury alters the temporal and spatial distribution of redox signaling

Although excessive keratinocyte movement following thermal injury did not immediately damage sensory neurons, we speculated that this behavior may induce long-term damage by altering the physical or biochemical composition of the wound microenvironment. To test this hypothesis, we next sought a method to limit injury induced keratinocyte movement. Previous studies have demonstrated that the presence of an osmotic gradient promotes keratinocyte migration via cell swelling[45]. Under control conditions, zebrafish are kept in water hypotonic to their interstitial fluid. Removing this osmotic gradient by wounding larvae in the presence of medium that is isotonic to the interstitial fluid has previously been shown to inhibit keratinocyte migration following mechanical injury[42,45]. We found that the presence of an isotonic solution also prevented the rapid movement of keratinocytes in response to a burn. Within the first hour following burn injury, keratinocyte average speed was reduced from 0.059 μm/s in control medium to 0.003 μm/s in isotonic medium (**Fig. 4A-C; Fig. S2C; Supplemental Movie 4**). Using isotonic medium, we next asked whether keratinocyte movement alters epidermal structure following burn injury. To visualize the epidermis, we used *Tg(Krt4:Lifeact-mRuby;LamC1:sfGFP)* larvae that express the actin probe Lifeact in keratinocytes and GFP-tagged laminin in the basement membrane. In uninjured larvae, the epidermis is characterized by two layers of tightly adhered keratinocytes resting on a flat sheet of laminin[39]. Following burn injury, we observed epidermal damage in burn wounded larvae that coincided temporally with the peak in axonal damage (**Fig. 4D**). While this damage was largely confined to the site of the original burn wound, it was characterized by the presence of delaminated keratinocytes clustering beyond the underlying laminin, which itself had become heavily folded. In contrast, larvae burned in the presence of isotonic medium exhibited almost no keratinocyte clustering with minimal extension beyond the underlying basement membrane (**Fig. 4D**). This suggests that early movement of keratinocytes following burn injury mediates the accumulation of tissue damage in the long term.

Repair of wounds relies on coordinated ROS production by epithelial cells [45–47]. Following mechanical injuries, such as tailfin transection or laser ablation, transient and localized H_2O_2 promotes sensory neuron regeneration[20,48]. Because of this, we hypothesized that the excessive keratinocyte movement and sustained damage in burn tissue may result in dysregulated ROS production and contribute to sensory neuron damage. To test this, we quantified H_2O_2 level in larvae burned in either control or isotonic medium using the fluorescent

dye pentafluorobenzenesulfonyl fluorescein (Pfbsf). Immediately following burn injury, the level of H_2O_2 was the same between the treatment groups, indicating that cells wounded in the presence of isotonic medium maintain their normal ability to generate ROS (**Fig. 4E, F**)[47]. At 6 hours post burn, we found that H_2O_2 production was no longer localized to the wound edge in control burned larvae and spread throughout the tailfin. By contrast, H_2O_2 remained restricted to the wound edge in larvae burned in the presence of isotonic medium and displayed a similar localized pattern to that observed after mechanical injury[46,49]. Quantification revealed that H_2O_2 level at the wound edge was similar between control and isotonic treated larvae 6 hpb. However, the levels of H_2O_2 were approximately 6-fold lower in the fin epithelial tissue adjacent to the burn wound with isotonic treatment (**Fig. 4E, G**). These findings suggest that excessive keratinocyte movement, and the resulting epidermal damage, generate an oxidative environment at the tissue-scale that leads to sustained sensory neuron damage after burn.

Isotonic media is sufficient to rescue sensory neuron regeneration and function after burn

To determine if keratinocyte movement contributes to sustained neuronal damage, we assessed axonal damage and regeneration in burned larvae treated with isotonic medium to prevent keratinocyte movement. Immediately following injury, larvae burned in isotonic medium displayed axonal damage similar to larvae injured in control medium (**Fig. 5A**). However, 6 hpb, axonal damage in isotonic treated larvae remained restricted to the site of injury, similar to the spatially restricted H_2O_2 signal induced by isotonic treatment (**Fig. 5A**). We also found that isotonic media reduced axonal damage and restored sensory neuron regeneration and function. Accordingly, larvae burned in isotonic medium had significantly greater axon density 24 hpw (**Fig. 5B, D**), and more than 85% of isotonic treated larvae had restored sensory function at 24 hpb (**Fig. 5E**). To determine if the benefit of isotonic solution was due to its ionic composition, we tested whether an isotonic solution of the sugar D-Sorbitol had similar effects. We also found that isotonic solutions made using D-Sorbitol treatment limited basal keratinocyte migration and restored axon density and sensory function after burn (**Fig. S2F-H**). Since keratinocyte movement occurs early after injury, within the first hour after burn, we determined if treatment with isotonic solution after keratinocyte movement had already occurred was sufficient

to improve neuronal regeneration. If isotonic medium was added 1 hpw, after the migration was complete, we found no improvement in sensory axon density or function 24 hpb, supporting the idea that early wound events during the first hour are critical for their effects on sensory neuron function (**Fig. 5C, F, G**). Collectively, these findings suggest that early keratinocyte movement after burn coordinates spatial redox signaling that is needed for efficient sensory neuron regeneration.

Elevated wound-associated ROS causes sensory neuron damage independent of epithelial cell dynamics

To determine if elevated wound-associated ROS in the absence of keratinocyte movement was sufficient to induce neuronal damage, we next tested whether increasing ROS production in the presence of isotonic solution was sufficient to induce axonal damage and impair sensory neuron function after burn. For this, we treated larvae with the NADPH oxidase activator Phorbol-12-Myristate-13-Acetate (PMA) in the presence and absence of isotonic media for 6 hpb. Due to the documented toxicity of PMA[50], we limited our treatment to 6 hpb, similar to the timeframe in which we observed accumulating axonal damage in burned fish. To maintain consistency in our treatments, larvae were only placed in isotonic solution for 6 hpb, which was sufficient to restore neuronal function after burn in the absence of PMA (**Fig. S3A, B**). Addition of PMA to isotonic solution increased H_2O_2 throughout the epithelium following burn injury (**Fig. S3C**), but did not affect wound induced keratinocyte movement or epithelial damage 6 hpb (**Fig. 6A-C; Fig. S2D**). PMA treatment in burned larvae in the presence of isotonic treatment increased axonal damage (**Fig. 6D**). Quantification of axon regeneration 24 hpw showed that larvae treated with PMA had 53.9±0.06% of the axon density of larvae burned in only isotonic medium (**Fig. 6E, F**). This defect was associated with significantly impaired sensory neuron function (**Fig. 6G**). Taken together, these findings suggest that excessive ROS mediates neuronal damage independent of keratinocyte movement in burned tissue.

To determine if limiting ROS after burn was sufficient to rescue neuronal function, we used N-Acetyl Cysteine (NAC), a commonly used antioxidant previously shown to reduce ROS in zebrafish and available for use in humans[51,52]. Treatment with NAC had no effect on keratinocyte movement and did not prevent long-term epithelial damage associated with burn injury (**Fig. 6H-J; Fig. S2E**). Despite this, NAC treatment improved

axonal damage 6 hpb (**Fig. 6K**), and axon regeneration with a nearly 2-fold increase in the percentage of larvae sensitive to touch (**Fig. 6L-N**). Taken together, these findings suggest that regulated keratinocyte movement mediates spatial restriction of ROS signaling that promotes sensory neuron regeneration after burn injury.

Discussion

Tissue repair requires the coordination of signaling across spatial and temporal scales. Our prior work showed that early ROS signaling immediately after mechanical damage is necessary for longer term tissue repair[53]. Wound-induced ROS production is also required for leukocyte recruitment, ECM remodeling, and sensory neuron regeneration in response to tissue injury[20,29,54,55]. While the requirement of ROS production following tissue injury is clear, we lack an understanding of how early redox signaling is coordinated temporally and spatially to mediate long-term tissue repair. We recently reported that thermal injury induces a distinct repair response with impaired collagen remodeling and delayed healing[27,29]. In light of the known defect in sensory neuron function after burn injuries in humans, we sought to determine how the early epithelial response modulates sensory neuron function. Our findings suggest that early damage-induced keratinocyte movement plays a role in the spatial patterning of ROS production in the wound microenvironment that impacts sensory neuron regeneration.

Collective keratinocyte migration is conserved across species and is required to mediate wound closure after tissue injury[56,57]. While collective cell migration has been observed in larval zebrafish previously[58,59], its contribution to epithelial repair remains unclear. In comparison to the organized movement associated with keratinocyte response to mechanical injury, our observations here identify excessive keratinocyte movement as a defining feature of the response to thermal injury. In addition to cell movement continuing for significantly longer after injury, keratinocyte movement following thermal injury appeared to lack a stereotypical leader-follower dynamic, with cells instead moving independently of one another but as a collective group. This observation suggests that collective keratinocyte migration is a feature of tissue repair in larval zebrafish regardless of the mode of injury and that its regulation is required for the success of long-term healing.

Recent evidence points to osmotic regulation in the control of wound-induced keratinocyte migration in larval zebrafish[45]. Zebrafish naturally exist in water that is hypotonic to the interstitium. Influx of fluid down an osmotic gradient following breach of the epithelial barrier results in cell swelling, which is prevented by wounding in isotonic solution[60]. Cell swelling is thought to induce migration by promoting branched actin polymerization and lamellipodia formation[61–63], likely through the activity of mechanically-activated ion channels. Our results also show that osmotic modulation is critical for keratinocyte motility in response to burn injury, suggesting it may provide a key mechanism that governs collective epithelial cell migration. We find that the excessive keratinocyte movement induced by thermal injury is significantly limited by wounding in isotonic solution. Interestingly, limiting keratinocyte motility by isotonic treatment is detrimental to tissue repair following mechanical injury[45], but we find that isotonic treatment rescues both epithelial morphology and sensory neuron regeneration following thermal injury. This suggests that there is an optimal amount of keratinocyte movement needed for successful repair and long-term regeneration. Interestingly, our findings suggest that the role of keratinocyte motility in sensory neuron damage is not immediate because we saw no evidence of neuronal damage during migration. Instead, the onset of axonal damage appears after keratinocyte movement has abated. These observations raised the possibility of an alternate role for keratinocyte movement in controlling sensory neuron damage and repair.

A conceptual challenge in wound repair has been understanding how early wound-induced events are linked to long-term repair[64]. ROS signaling provides a framework to understand this link due to its requirement for mediating both early wound contraction and long-term regeneration. In zebrafish, the reactive oxygen species H_2O_2 is generated along a tissue-scale gradient with the highest levels at the wound edge[55]. While this spatial gradient undoubtedly directs cell function based on the position along the gradient, uncontrolled ROS production is damaging to tissues. Therefore, a mechanism must exist to control ROS such that it remains relatively localized to the site of damage and is controlled temporally and spatially. In addition to their early role in wound resealing, keratinocyte redox signaling is critical for long-term repair. In addition to its role in

controlling migration, osmotic modulation is known to affect the long-term signaling of keratinocytes following tissue injury. Cell swelling induces cPLA$_2$-dependent LTB$_4$ production and immune cell recruitment[65]. This suggests the signals that control keratinocyte motility may simultaneously modify long-term keratinocyte signaling.

Here we found that thermal injury altered the spatial profile of H_2O_2 production. Immediately following injury, H_2O_2 production is primarily localized to the wound edge, similar to the response to mechanical injury. However, thermal injury causes H_2O_2 production to spread over time. Strikingly, limiting keratinocyte motility by wounding in isotonic solution spatially restricted H_2O_2 production in a pattern similar to mechanical injury, suggesting that keratinocyte movement may serve as a mechanism to spatially control ROS signaling during tissue repair. Importantly, in agreement with results of others, we found that isotonic treatment did not alter the capacity of cells to produce ROS[65], with similar H_2O_2 levels in the wound region in control and isotonic conditions. Further, our data suggest that the effect of spatially limiting ROS production on long-term sensory neuron regeneration is dependent on keratinocyte motility. When keratinocyte movement was allowed to occur for 1 hour after wounding and then the fin was isotonic-treated, we observed no improvement in sensory neuron regeneration. This suggests that regulating early keratinocyte motility is important for longer-term wound signaling and sensory neuron regeneration.

The benefit of a system in which keratinocyte motility controls downstream signaling is two-fold. First, it enables signaling to be scaled to the size of injury. If more cells migrate due to a larger injury, then production of ROS will likewise increase. Second, this system provides a mechanism to control the spatial localization of signaling. Keratinocyte migration requires transiently detaching from neighboring cells. Thus, the act of migrating induces a physical change in the tissue that demarcates the wound region from healthy tissue. It is known that production of ROS promotes keratinocyte motility, and that adhesion is linked to cellular redox state[13,66]. Given these observations, it seems plausible that ROS production in wounded tissue is linked to the biomechanical state of keratinocytes – with low ROS in static, adhered cells, and high ROS in loosely

adhered or migrating cells. A conceptual framework such as this would explain excessive ROS production in burn wounded tissue. Early keratinocyte dynamics in burned tissue are associated with normal wound edge ROS production. However, lack of a migratory stop signal may result in excessive keratinocyte migration and subsequent epithelial damage associated with keratinocytes detaching from the basal lamina. Therefore, failure to restore epithelial homeostasis due to unabated keratinocyte movement may allow for ROS production to continue over time and spread further away from the wound site. Future studies will be aimed at identifying the molecular link between cell migration and ROS production during tissue repair.

Burn wounded patients have poor prognosis and frequently suffer from chronic pain and altered sensory perception[23–26,67,68], indicating a defect in the regenerative capacity of the peripheral sensory nervous system after burn. A roadblock to developing better treatments to improve sensory outcomes or burn wound healing in general is our lack of understanding of underlying wound pathophysiology[69]. We previously showed that burn wounding of larval zebrafish recapitulates key features of burn wound pathology in humans[27,29]. The current findings suggest that controlling redox balance may provide a potential treatment for burn wounds. While we must acknowledge the potential off-target effects of the drugs used to modify ROS production in our study, PMA and NAC[50–52,70–73], these findings further implicate a key role for a balance in ROS signaling during tissue repair.

In summary, we have identified early wound-induced keratinocyte movement as a mechanism that controls spatial patterning of long-term wound signaling. These findings highlight the ability of keratinocytes within the wound microenvironment to integrate early signaling and migratory functions that mediate initial wound closure and subsequently regulate spatial tissue signaling necessary for efficient sensory neuron regeneration. Further, our results not only highlight the utility of larval zebrafish for revealing new insights of the tissue response to injury *in vivo*, but also demonstrate the potential for these findings to inform new treatment strategies for wound healing more broadly.

Materials & Methods

Ethics

This study was carried out in accordance with the recommendations from the Guide for the Care and Use of Laboratory Animals from the National Institutes of Health. All zebrafish protocols in this study were approved by the University of Wisconsin-Madison Research Animals Resource Center (Protocol M005405-R02).

Zebrafish Maintenance and Handling

Adult zebrafish and embryos were maintained as described previously[27,74]. For all experiments, 3 days post-fertilization larvae were anesthetized in E3 medium containing 0.2 mg/mL Tricaine (ethyl 3-aminobenzoate; Sigma-Aldrich). All transgenic lines including *Tg(Ngn1:GFP-Caax)*[31], *Tg(Krt4:LifeAct-mRuby)*[75], *Tg(Krt4:Utrophin-GFP), Tg(Krt4:TdTomato), TgBac(Lamc1:Lamc1-sfGFP)*[59], *Tg(ElavI3:GCaMP5)*[76], *Tg(Krtt1c19e:LifeAct-mRuby),* and *Tg(Krtt1c19e:acGFP)* were maintained on the AB background strain. To screen larvae for fluorescence, a Zeiss Zoomscope EMS3/SyCoP3 with a Plan-NeoFluar Z objective was used.

Generation of Tg(Krtt1c19e:LifeAct-mRuby) Transgenic Line

The *Krtt1c19e* promoter[40] flanked by Age1 and NotI was isolated and cloned into an expression vector containing Lifeact-mRuby and Tol2 elements for genomic integration. 25 ng/µL of construct and 50 ng/µL transposase mRNA were injected into the yolk of one-cell stage embryos. F_0 larvae were raised to adulthood and crossed to adult AB zebrafish. F_2 larvae were screened for Ruby expression and grown to generate stable lines. *Tg(Ngn1:GFP-Caax)* larvae transiently expressing *Krtt1c19e:Lifeact-m*Ruby were used for simultaneous imaging of neuron-keratinocyte interactions.

Caudal Fin Transection and Burn Injury

Transection of the caudal fin was performed on anesthetized larvae in a 60 mm tissue culture-treated dish containing E3 with Tricaine. Larvae were cut perpendicular to the caudal notochord boundary using a surgical

blade (Feather No. 10, VWR). Burn injury was performed on anesthetized larvae in a 60 mm tissue culture-treated dish containing E3 with Tricaine. A fine tip cautery pen (Geiger Medical Technologies) was used to burn the caudal fin until the wounded area bordered but did not touch the posterior notochord boundary. After injury, larvae were placed into new 60 mm dishes with E3 and maintained at 28.5 C until imaging. To two-wound experiments, larvae were either transected or burned as described above with the exception that injury was applied halfway to the notochord boundary to leave adequate room for secondary transection. Secondary transection, after either 5 minutes or 6 hours, was performed as described above.

Drug Treatment

For all treatments, larvae were incubated in the indicated drug solution for 15-30 minutes. Unless indicated otherwise, larvae were in the presence of treatment for the duration of all experiments. Isotonic medium was prepared by supplementing E3 medium with either NaCl (Fisher Scientific) or D-Sorbitol (Sigma-Aldrich) to a final concentration of 135 mM. Isotonic medium does not noticeably impair embryonic development or health of the larvae or the time scale used here[45,46]. Experiments using N-Acetyl Cysteine (NAC, Sigma-Aldrich) were performed at 100 µM final concentration. For experiments using Phorbol-12-Myristate-13-Acetate (PMA, Sigma-Aldrich), larvae were incubated in 50 nM PMA in the presence of Isotonic NaCl E3 medium. Larvae were washed into fresh E3 medium 6 hours post-wound.

Live and Time-lapse Imaging

Larvae were imaged using a spinning disc microscope (CSU-X, Yokogawa) with a confocal scanhead on a Zeiss Observer Z.1 inverted microscope, Plan-Apochromat NA 0.8/20X objective, and a Photometrics Evolve EMCCD camera. All images were acquired using ZEN 2.6 software. For time lapse imaging, larvae were mounted in a zWEDGI restraining device[77] with the head being covered in 2% low-melting point agarose (Sigma-Aldrich). For single time point imaging, anesthetized larvae were mounted in 2% low-melting point agarose on a 35 mm glass-bottom depression dish (CellVis). In all cases, larvae were imaged in E3 medium supplemented with Tricaine as described above.

Quantification of Axon Density and Sensory Function

Axon density was measured by generating maximum intensity z-projected images of the caudal fin using FIJI[78]. The caudal fin area posterior to the notochord was outlined using the Polygon tool and measured to obtain a total surface area ROI. Axons inside the outlined area were manually thresholded so all axons posterior to the notochord were labeled and no saturated pixels were present. Density was measured by dividing the area of detected axons by the area of the ROI. In each case, density values of the experimental sample were normalized to the indicated control, either unwounded or control treated fins. Sensory neuron function was determined using a behavioral touch assay[33]. 3-day post-fertilization larvae were wounded as described above. At the indicated time post-wound, larvae were briefly anesthetized for mounting into the zWEDGI restraining device, with only the head being mounted in 2% low-melting point agarose. Fresh E3 was added and larvae were allowed to rest for one hour. To assess sensory function, the wounded region of caudal fin was touched with the tip of an eyelash brush (No. 1 Superfine Eyelash, Ted Pella) and the presence or absence of a twitch reflex was recorded.

Visualization of Sensory Neuron and Tissue Damage

To visualize damage to sensory neurons, *Tg(ElavI3:GCaMP5)* larvae were used. Representative images are maximum intensity z-projections of the caudal fin generated using FIJI. FM 1-43 dye (Life Technologies) was used to visualize tissue damage following transection and burn injury. For this, larvae were incubated in 1 mg/ml FM 1-43 for 15 minutes prior to injury. Larvae were maintained at 28.5 C until imaging at the indicated time post-injury.

Quantification of Hydrogen Peroxide Level

Hydrogen peroxide was quantified using pentafluorobenzenesulfonyl fluorescein (Pfbsf, Santa Cruz)[79]. Larvae were incubated in 1 µM Pfbsf for 15 minutes prior to injury and maintained in dye solution for the duration of each experiment. Pfbsf intensity was calculated by generating sum projections and measuring mean gray value

in FIJI. For measurements based on localization within the fin, the posterior tip of the notochord was used to denote the interface between the wound zone and fin zone.

Cell Tracking

Basal keratinocyte tracking following tissue injury was performed using *Tg(Krtt1c19e:acGFP)* larvae. Cell tracking was performed using the Spots module in Imaris version 9.8.2 (Bitplane, Zurich, Switzerland). For each larva, 3 representative cells were identified and manual tracking was performed, with the average of these cells being used to generate a single value for further analysis. To control for drift of the entire fin during imaging, non-moving pigment was manually tracked by Brightfield and track length was subtracted from basal keratinocyte movement. In all cases, larvae were imaged for 1 hour following injury at an interval of 30 seconds.

Morpholino Injection

Ngn1 morpholino with the sequence 5'-ACG ATC TCC ATT GTT GAT AAC CTG G-3'[80] was used to prevent sensory neuron formation in Elavl3-GCaMP5 larvae. 5 ng of Ngn1 morpholino was injected into the yolk of one- to two-cell stage zebrafish embryos. Larvae were incubated at 28.5 C until used for experiments at 3 days post-fertilization. Before use in experiments, larvae were screened by the sensory function assay described above to ensure that sensory neurons were depleted.

Image Processing

Images were processed and analyzed using FIJI and Imaris version 9.8.2 (Bitplane, Zurich, Switzerland) as indicated. Supplemental movies were generated in FIJI and edited using Adobe Premiere Pro (Adobe). In Adobe Premiere Pro, pseudocoloring of individual keratinocytes was done using the Color Effects module with manual tracking.

Statistical Analysis

Each experimental condition consists of at least three independent biological replicates, defined as three clutches of larvae spawned on three different days. Cell-tracking experiments were analyzed using non-parametric methods (Wilcoxon rank-sum test). Quantification of axon density was analyzed using linear mixed-effect models in which biological replicate was treated as a random effect and experimental conditions (e.g., wound, time, or chemical treatment) treated as fixed factors. Experiments measuring fluorescence intensity (Pfbsf intensity) were analyzed in the same manner, except the response (fluorescence) was log-transformed prior to analysis. Means computed on the log scale estimate the median response when back transformed to original units. At the same time, differences between means (of log-transformed data) become ratios of medians after back transformation to the original scale[81]. Experiments involving the proportion of fish that responded to touch were analyzed using a general linear model that included replicate and experimental condition as fixed effects; standard errors used for estimation and testing were adjusted to correct for heteroscedasticity in the proportions[82]. Graphing was performed using GraphPad Prism 9 (GraphPad Software, Inc, San Diego, CA). Sample size is reported for specific experiments in the figure legends.

Acknowledgements

We would like to thank Dr. Mary Halloran (University of Wisconsin-Madison) for the gift of the *Tg(Ngn1-GFP-Caax)* fish line, Dr. Jan Huisken (University of Göttingen) for the *Tg(Elavl3-GCaMP5)* fish line, Dr. Alvaro Sagasti (University of California Los Angeles) for the *Tg(Krtt1c19e:acGFP)* fish line, and Dr. Holger Knaut (New York University) for the *TgBac(LamC1:LamC1-sfGFP)* fish line. We would like to thank Michael Lasarev for his contribution to statistical analysis, Taylor Schoen and Veronika Miskolci for their critical reading of the manuscript, and the members of the Huttenlocher lab for their thoughtful input throughout this project. The authors acknowledge K99 GM147303 to Adam Horn and R35 GM118027 to Anna Huttenlocher.

Author Contributions

A. Fister, A. Horn, and A. Huttenlocher designed and planned the experimental approach. A. Fister and A. Horn performed all the experiments. A. Fister, A. Horn, and A. Huttenlocher wrote the paper.

Declaration of Interests

The authors declare no competing financial interests.

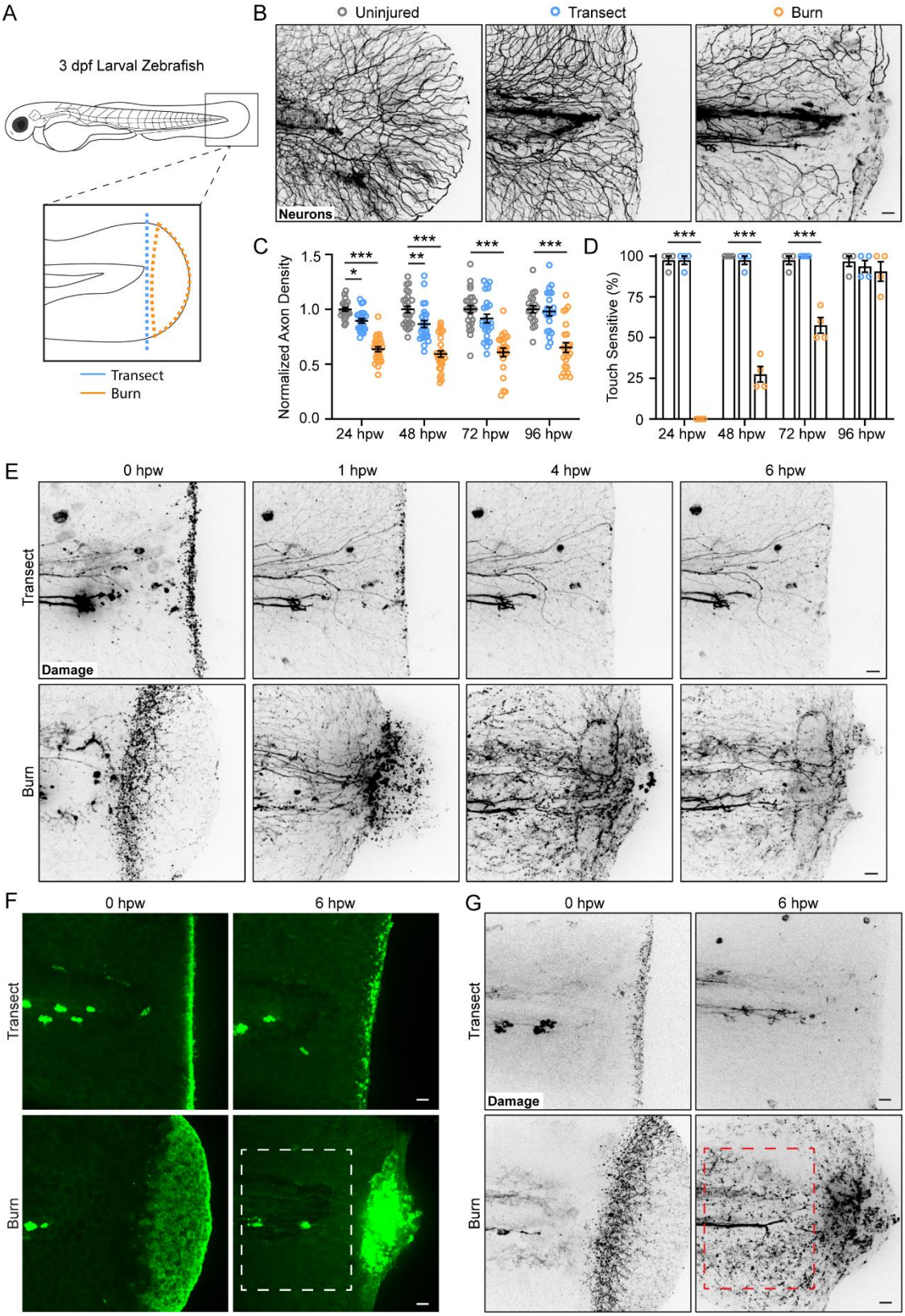

Figure 1: Peripheral sensory neurons have impaired regeneration after burn injury. (A) Schematic of larval zebrafish injury. (B) Images of sensory neurons in uninjured, transected, and burned *Tg(Ngn1:GFP-*

Caax) caudal fins. (C) Quantification of axon density for uninjured, transected, and burned larvae in the wound area 24-96 hpw. N>20 larvae per condition. (D) Quantification of sensory perception for uninjured, transected, and burned larvae 24-96 hpw. N>32 larvae per condition from 4 independent experiments. (E) Time series images of axonal damage, indicated by calcium-positive punctae (black dots), in *Tg(Elavl3:GCaMP5)* larvae following either transection or burn injury. (F) Images of larvae either transected or burned in the presence of FM 1-43 dye. White dashed box denotes area of uninjured tissue in which axonal damage appears in (G). (G) Images show axonal damage following transection or burn injury. Red dashed box corresponds to the tissue region highlighted in F. In all cases, scale bars=20 μm. *p<0.05, **p<0.01, ***p<0.001.

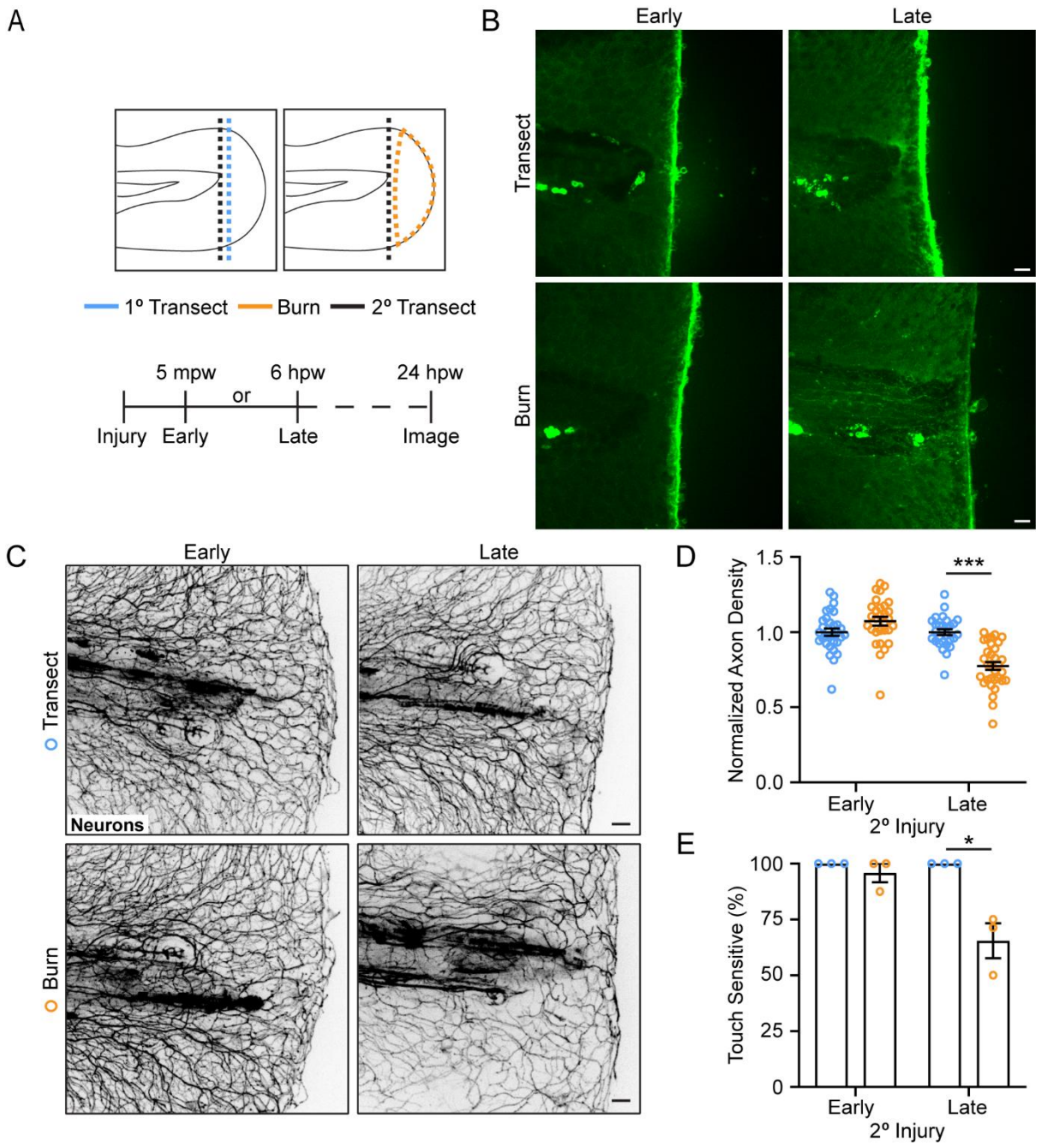

Figure 2: The burn wound microenvironment contributes to impaired sensory neuron regeneration. (A) Schematic of two-wound experiment design. (B) Images of characteristic FM dye staining following secondary transection in the two-wound experiment. Scale=20 µm. (C) Images of sensory neurons in larvae subjected to an initial transection or burn injury followed by subsequent transection either early (5 mpw) or late (6 hpw). (D) Quantification of axon density in wounded tissue 24 hpw from larvae wounded as in B. N>28 larvae per

condition. (E) Quantification of sensory perception in wounded tissue 24 hpw from larvae wounded as in B. N=24 larvae each from 3 independent experiments. In all cases, scale bars=20 μm. *$p<0.05$, ***$p<0.001$.

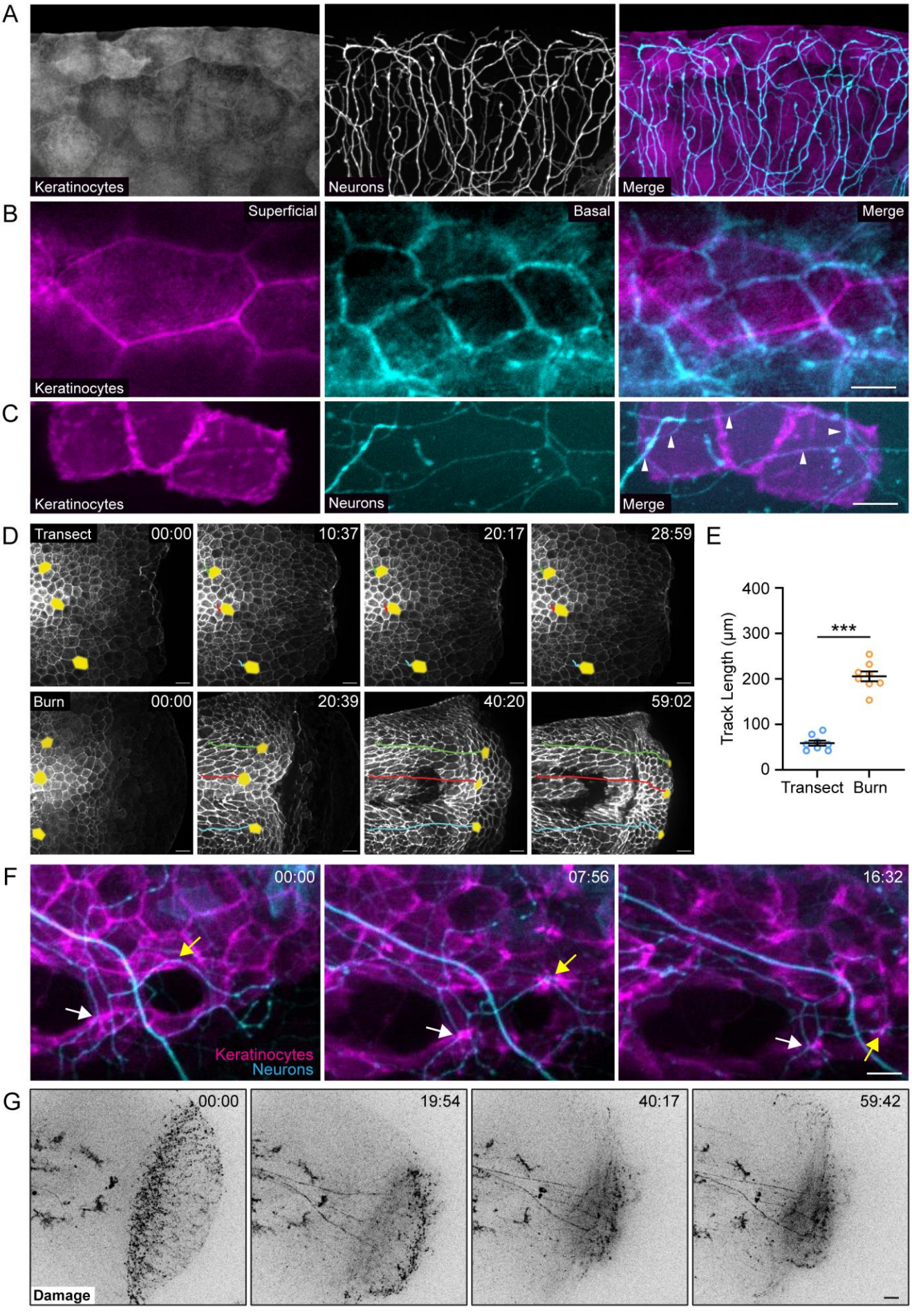

Figure 3: Burn injury induces coordinated keratinocyte and sensory neuron movement. (A) Images of sensory neurons, *Tg(Ngn1:GFP-Caax)*, and keratinocytes, *Tg(Krt4:TdTomato)*, in the larval zebrafish epidermis. Scale = 20 µm. (B) Images of superficial (left) and basal (middle) keratinocytes from 3 days post-fertilization *Tg(Krt4:Lifeact-Ruby)* larvae. Images were isolated from the same Z-stack separated by 5.44 µm (Collected at a z-interval of 0.68 µm). Scale=10 µm. (C) Images show regions of co-localization (arrowhead) between sensory neurons, *Tg(Ngn1:GFP-Caax)* and basal keratinocytes, *Tg(Krtt1c19e:Lifeact-Ruby)*. Scale=10 µm. (D) Time-series images of *Tg(Krt4:Utrophin-GFP)* larvae after either transection or burn injury. Yellow pseudocolored cells and colored tracks highlight keratinocyte displacement. (E) Distance of keratinocyte movement over 1 hpw. N= 8 larvae each. (F) Time-series images of sensory neuron and basal keratinocyte-labeled larvae post-burn. Arrowheads highlight coincident movement between keratinocytes and associated sensory neurons. Scale bar=10 µm. (G) Time-series images of calcium flux in neurons as an indicator of axonal damage following burn injury in *Tg(Elavl3:GCaMP5)* larvae. In all cases, scale bars=20 µm. *$p<0.05$, ***$p<0.001$.

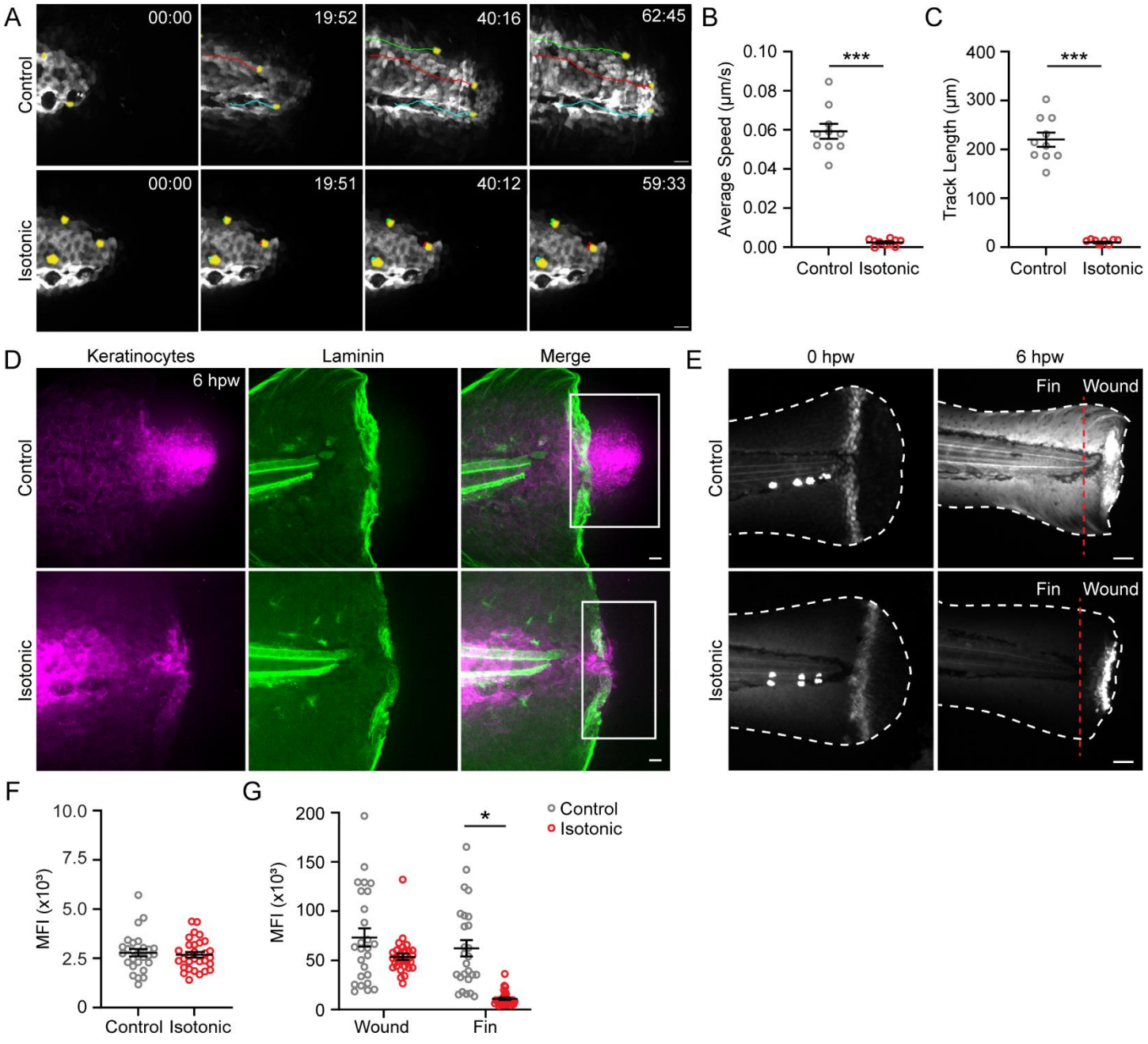

Figure 4: Dysregulated keratinocyte movement causes sustained epidermal damage and loss of localized reactive oxygen species signaling. (A) Time-series images of basal keratinocyte movement in *Tg(Krtt1c19e:acGFP)* larvae after burn injury in the indicated treatment. (B) Plot of basal keratinocyte average speed over 1 hpw treated as in A. N=10 larvae each. (C) Distance of keratinocyte movement over 1 hpw treated as in A. N=10 larvae each. (D) Images of *Tg(Krt4:Lifeact-Ruby;LamC1:GFP)* larvae 6 hours after burn injury. (E) Images of hydrogen peroxide level (Pfbsf intensity) following burn injury. Dashed red line denotes the boundary between the wound area and distal fin tissue. Scale bar=50 μm. (F) Quantification of Pfbsf intensity

(Mean Fluorescence Intensity) immediately (0 hpw) after burn injury. N=27 control and 30 treated larvae. (G) Quantification of Pfbsf intensity (Mean Fluorescence Intensity) 6 hpw in the indicated region of the fin. N=26 control and 31 treated larvae. Unless otherwise indicated, scale bars=20 μM. *$p<0.05$, ***$p<0.001$.

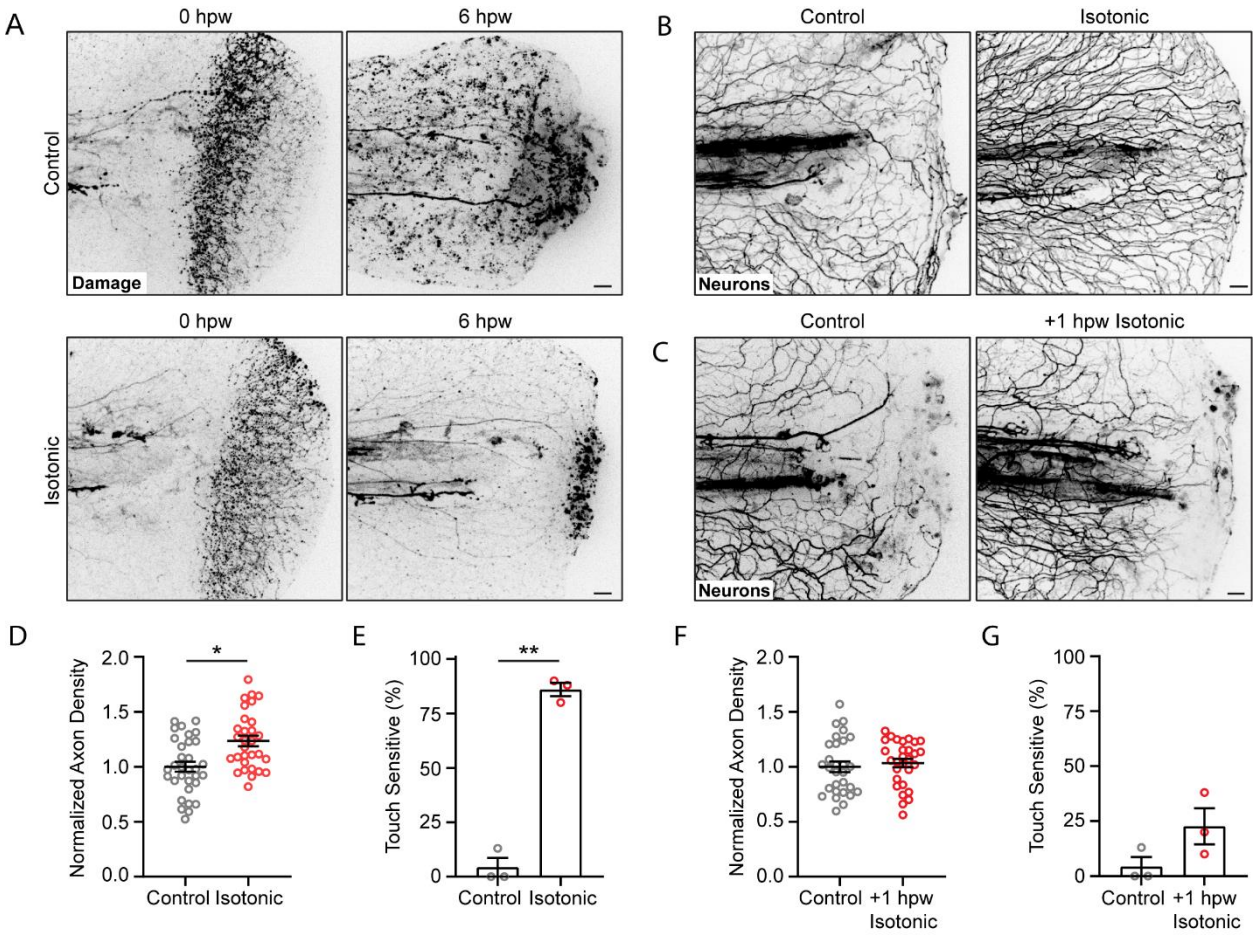

Figure 5: Excessive keratinocyte movement immediately after burn injury impairs sensory neuron regeneration. (A) Images of axonal damage in control or isotonic treated *Tg(Elavl3:GCaMP5)* larvae 0 or 6 hpw. (B) Images of sensory neurons in control larvae or isotonic treated larvae 24 hpw. (C) Images of sensory neurons 24 hpw in control or isotonic treated larvae starting 1 hpw. (D) Quantification of axon density 24 hpw in larvae treated as depicted in B. N=32 control and 30 treated larvae. (E) Quantification of sensory perception 24 hpw in larvae treated as in B. N=24 larvae each from 3 independent experiments. (F) Quantification of axon density 24 hpw in larvae treated as in C. N=29 larvae each. (G) Quantification of sensory perception 24 hpw in larvae treated as in C. N=28 larvae each from 3 independent experiments. Unless otherwise indicated, scale bars=20 µm. *p<0.05, **p<0.01.

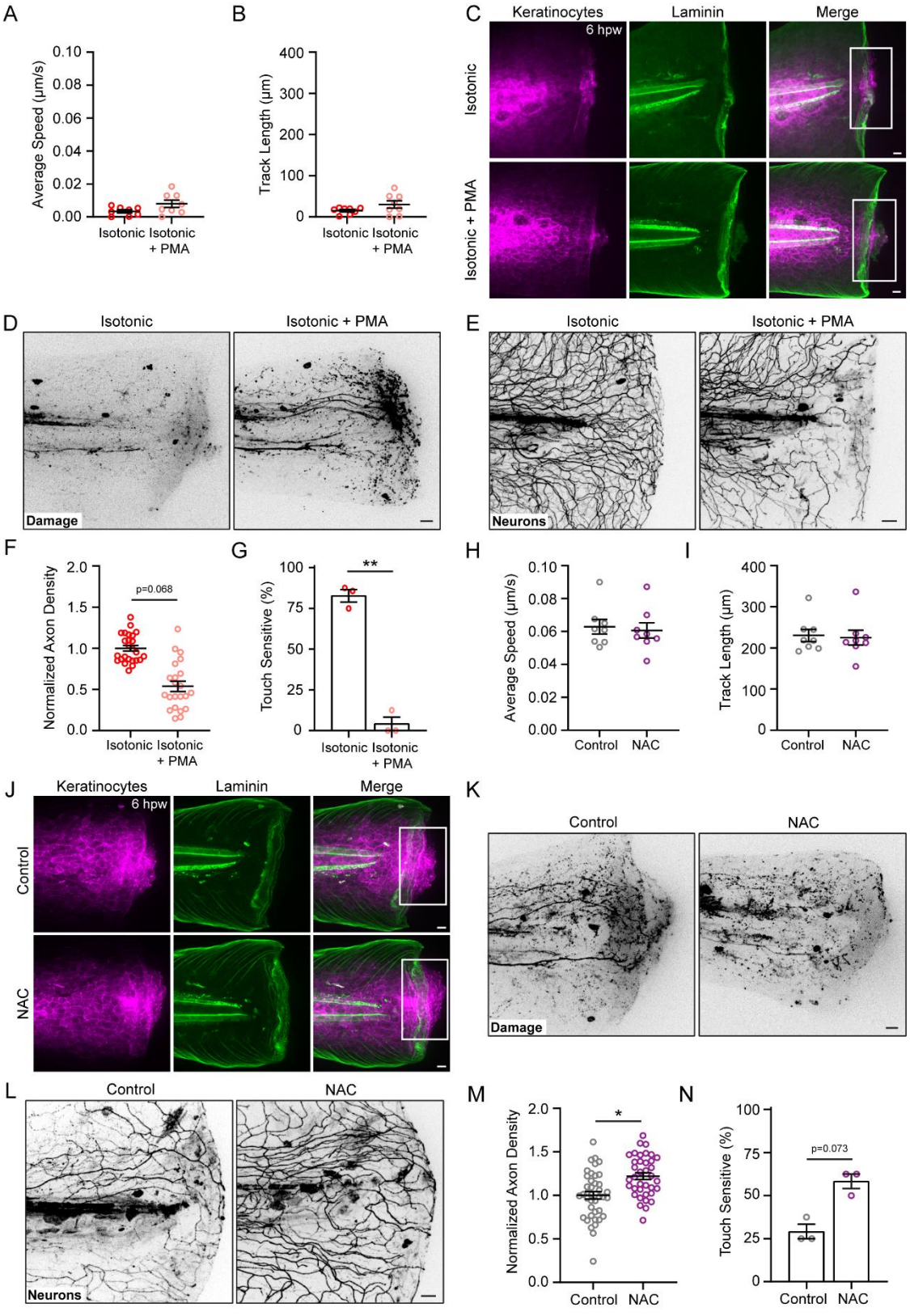

Fig. 6: Elevated wound-induced ROS causes sensory neuron damage independent of epithelial tissue dynamics. (A) Plot of basal keratinocyte average speed over 1 hpw in isotonic medium with or without PMA.

N=8 larvae each. (B) Distance of keratinocyte movement over 1 hpw treated as in A. N=8 larvae each. (C) Images of *Tg(Krt4:Lifeact-Ruby;LamC1:GFP)* larvae 6 hpw. (D) Images of axonal damage 6 hpw in larvae wounded in isotonic medium with or without PMA. (E) Images of sensory neurons 24 hpw in larvae wounded in isotonic medium with or without PMA. (F) Quantification of axon density 24 hpw in larvae treated as in E. N=25 control and 22 treated larvae. (G) Quantification of sensory perception 24 hpw in larvae treated as in E. N=23 control and 21 treated larvae from 3 independent experiments. (H) Plot of basal keratinocyte average speed over 1 hpw in control or NAC treated larvae. N=8 larvae each. (I) Distance of keratinocyte movement over 1 hpw treated as in H. N=8 larvae each. (J) Images of *Tg(Krt4:Lifeact-Ruby;LamC1:GFP)* larvae 6 hpw. (K) Images of axonal damage 6 hpw in control or NAC treated larvae. (L) Images of sensory neurons in control or NAC-treated larvae 24 hpw. (M) Quantification of axon density 24 hpw in larvae treated as in L. N=40 control and 37 treated larvae. (N) Quantification of sensory perception 24 hpw in larvae treated as in L. N=24 larvae each from 3 independent experiments. In all cases, scale bars=20 μm. *$p<0.05$, **$p<0.01$.

References

1. DiAntonio, A. (2019). Axon degeneration: mechanistic insights lead to therapeutic opportunities for the prevention and treatment of peripheral neuropathy. Pain *160*, S17–S22. 10.1097/J.PAIN.0000000000001528.
2. Li, Y., Pazyra-Murphy, M.F., Avizonis, D., de Sá Tavares Russo, M., Tang, S., Chen, C.Y., Hsueh, Y.P., Bergholz, J.S., Jiang, T., Zhao, J.J., et al. (2022). Sarm1 activation produces cADPR to increase intra-axonal Ca++ and promote axon degeneration in PIPN. J Cell Biol *221*. 10.1083/jcb.202106080.
3. Rabiller, L., Labit, E., Guissard, C., Gilardi, S., Guiard, B.P., Moulédous, L., Silva, M., Mithieux, G., Pénicaud, L., Lorsignol, A., et al. (2021). Pain sensing neurons promote tissue regeneration in adult mice. NPJ Regen Med *6*. 10.1038/s41536-021-00175-7.
4. Reyes, R., Haendel, M., Grant, D., Melancon, E., and Eisen, J.S. (2004). Slow Degeneration of Zebrafish Rohon-Beard Neurons during Programmed Cell Death. Developmental Dynamics *229*, 30–41. 10.1002/DVDY.10488.
5. Pope, H.M., and Voigt, M.M. (2014). Peripheral Glia Have a Pivotal Role in the Initial Response to Axon Degeneration of Peripheral Sensory Neurons in Zebrafish. PLoS One *9*, 103283. 10.1371/journal.pone.0103283.
6. Rasmussen, J.P., Sack, G.S., Martin, S.M., and Sagasti, A. (2015). Vertebrate Epidermal Cells Are Broad-Specificity Phagocytes That Clear Sensory Axon Debris. 10.1523/JNEUROSCI.3613-14.2015.
7. Mahar, M., and Cavalli, V. (2018). Intrinsic mechanisms of neuronal axon regeneration. Nat Rev Neurosci *19*, 323–337. 10.1038/S41583-018-0001-8.
8. Renthal, W., Tochitsky, I., Yang, L., Cheng, Y.C., Li, E., Kawaguchi, R., Geschwind, D.H., and Woolf, C.J. (2020). Transcriptional reprogramming of distinct peripheral sensory neuron subtypes after axonal injury. Neuron *108*, 128. 10.1016/J.NEURON.2020.07.026.
9. Liu, K., Tedeschi, A., Park, K.K., and He, Z. (2011). Neuronal Intrinsic Mechanisms of Axon Regeneration. https://doi.org/10.1146/annurev-neuro-061010-113723 *34*, 131–152. 10.1146/ANNUREV-NEURO-061010-113723.
10. Villegas, R., Martin, S.M., O, K.C., Carrillo, S.A., Sagasti, A., and Allende, M.L. (2012). Dynamics of degeneration and regeneration in developing zebrafish peripheral axons reveals a requirement for extrinsic cell types. Neural Dev *7*, 19. 10.1186/1749-8104-7-19.
11. Cheah, M., Fawcett, J.W., and Haenzi, B. (2017). Differential regenerative ability of sensory and motor neurons. Neurosci Lett *652*, 35–40. 10.1016/J.NEULET.2016.11.004.
12. Avraham, O., Feng, R., Ewan, E.E., Rustenhoven, J., Zhao, G., and Cavalli, V. (2021). Profiling sensory neuron microenvironment after peripheral and central axon injury reveals key pathways for neural repair. Elife *10*. 10.7554/ELIFE.68457.
13. Dunnill, C., Patton, T., Brennan, J., Barrett, J., Dryden, M., Cooke, J., Leaper, D., and Georgopoulos, N.T. (2015). Reactive oxygen species (ROS) and wound healing: the functional role of ROS and emerging ROS-modulating technologies for augmentation of the healing process. Int Wound J. 10.1111/iwj.12557.
14. Kuwabara, W.M.T., Zhang, L., Schuiki, I., Curi, R., Volchuk, A., and Alba-Loureiro, T.C. (2015). NADPH Oxidase-Dependent Production of Reactive Oxygen Species Induces Endoplasmatic Reticulum Stress in Neutrophil-Like HL60 Cells. PLoS One *10*. 10.1371/JOURNAL.PONE.0116410.
15. Sies, H., and Jones, D.P. (2020). Reactive oxygen species (ROS) as pleiotropic physiological signalling agents. Nature Reviews. 10.1038/s41580-020-0230-3.
16. Mittal, M., Siddiqui, M.R., Tran, K., Reddy, S.P., and Malik, A.B. COMPREHENSIVE INVITED REVIEW Reactive Oxygen Species in Inflammation and Tissue Injury. 10.1089/ars.2012.5149.
17. Linley, J.E., Ooi, L., Pettinger, L., Kirton, H., Boyle, J.P., Peers, C., and Gamper, N. (2012). Reactive oxygen species are second messengers of neurokinin signaling in peripheral sensory neurons. Proc Natl Acad Sci U S A *109*. 10.1073/PNAS.1201544109/-/DCSUPPLEMENTAL/PNAS.201201544SI.PDF.

18. Love, N.R., Chen, Y., Ishibashi, S., Kritsiligkou, P., Lea, R., Koh, Y., Gallop, J.L., Dorey, K., and Amaya, E. (2013). Amputation-induced reactive oxygen species (ROS) are required for successful Xenopus tadpole tail regeneration. Nat Cell Biol *15*, 222. 10.1038/NCB2659.
19. Montserrat, M., Romero, G., Mccathie, G., Jankun, P., Henry, &, and Roehl, H. (2018). Damage-induced reactive oxygen species enable zebrafish tail regeneration by repositioning of Hedgehog expressing cells. Nat Commun. 10.1038/s41467-018-06460-2.
20. Rieger, S., and Sagasti, A. (2011). Hydrogen Peroxide Promotes Injury-Induced Peripheral Sensory Axon Regeneration in the Zebrafish Skin. PLoS Biol *9*, 1000621. 10.1371/journal.pbio.1000621.
21. Cobb, C.A., and Cole, M.P. (2015). Oxidative and Nitrative Stress in Neurodegeneration HHS Public Access. Neurobiol Dis *84*, 4–21. 10.1016/j.nbd.2015.04.020.
22. Blais, M., Parenteau-bareil, R., Cadau, S., and Ois Berthod, F. Concise Review: Tissue-Engineered Skin and Nerve Regeneration in Burn Treatment. 10.5966/sctm.2012-0181.
23. Choinière, M., Melzack, R., and Papillon, J. (1991). Pain and paresthesia in patients with healed burns: An exploratory study. J Pain Symptom Manage *6*, 437–444. 10.1016/0885-3924(91)90043-4.
24. Tirado-Esteban, A., Seoane, J.L., Serracanta Domènech, J., Aguilera-Sáez, J., and Barret, J.P. (2020). Sensory alteration patterns in burned patients. Burns *46*, 1729–1736. 10.1016/J.BURNS.2019.08.005.
25. Pavoni, V., Gianesello, L., Paparella, L., Buoninsegni, L.T., and Barboni, E. (2010). Outcome predictors and quality of life of severe burn patients admitted to intensive care unit. Scand J Trauma Resusc Emerg Med *18*, 1–8. 10.1186/1757-7241-18-24/FIGURES/3.
26. Tsolakidis, S., Alharbi, Z., Rennekampff, H.O., Schmidhammer, M.R., Schmidhammer, R., and Rosenauer, R. (2022). "Out of Touch"—Recovering Sensibility after Burn Injury: A Review of the Literature. European Burn Journal *3*, 370–376. 10.3390/EBJ3020032/S1.
27. Miskolci, V., Squirrell, J., Rindy, J., Vincent, W., Sauer, J.D., Gibson, A., Eliceiri, K.W., and Huttenlocher, A. (2019). Distinct inflammatory and wound healing responses to complex caudal fin injuries of larval zebrafish. Elife *8*. 10.7554/ELIFE.45976.
28. LeBert, D.C., Squirrell, J.M., Rindy, J., Broadbridge, E., Lui, Y., Zakrzewska, A., Eliceiri, K.W., Meijer, A.H., and Huttenlocher, A. (2015). Matrix metalloproteinase 9 modulates collagen matrices and wound repair. Development (Cambridge) *142*, 2136–2146. 10.1242/DEV.121160/VIDEO-3.
29. LeBert, D., Squirrell, J.M., Freisinger, C., Rindy, J., Golenberg, N., Frecentese, G., Gibson, A., Eliceiri, K.W., and Huttenlocher, A. (2018). Damage-induced reactive oxygen species regulate vimentin and dynamic collagen-based projections to mediate wound repair. Elife. 10.7554/eLife.30703.001.
30. Andermann, P., Ungos, J., and Raible, D.W. (2002). Neurogenin1 Defines Zebrafish Cranial Sensory Ganglia Precursors. Dev Biol *251*, 45–58. 10.1006/DBIO.2002.0820.
31. Blader, P., Plessy, C., and Strähle, U. (2003). Multiple regulatory elements with spatially and temporally distinct activities control neurogenin1 expression in primary neurons of the zebrafish embryo. Mech Dev *120*, 211–218. 10.1016/S0925-4773(02)00413-6.
32. McGraw, H.F., Nechiporuk, A., and Raible, D.W. (2008). Zebrafish dorsal root ganglia neural precursor cells adopt a glial fate in the absence of neurogenin1. J Neurosci *28*, 12558–12569. 10.1523/JNEUROSCI.2079-08.2008.
33. Granato, M., van Eeden, F.J.M., Schach, U., Trowe, T., Brand, M., Furutani-Seiki, M., Haffter, P., Hammerschmidt, M., Heisenberg, C.P., Jiang, Y.J., et al. (1996). Genes controlling and mediating locomotion behavior of the zebrafish embryo and larva. Development *123*, 399–413. 10.1242/DEV.123.1.399.
34. Khaitin, A. (2021). Calcium in Neuronal and Glial Response to Axotomy. Int J Mol Sci *22*. 10.3390/IJMS222413344.
35. Linsley, J.W., Shah, K., Castello, N., Chan, M., Haddad, D., Doric, Z., Wang, S., Leks, W., Mancini, J., Oza, V., et al. (2021). Genetically encoded cell-death indicators (GEDI) to detect an early irreversible commitment to neurodegeneration. Nat Commun, 1–14. 10.1038/s41467-021-25549-9.

36. Arrázola, M.S., Saquel, C., Catalán, R.J., Barrientos, S.A., Hernandez, D.E., Martínez, N.W., Catenaccio, A., and Court, F.A. (2019). Axonal Degeneration Is Mediated by Necroptosis Activation. Journal of Neuroscience *39*, 3832–3844. 10.1523/JNEUROSCI.0881-18.2019.
37. Defour, A., Sreetama, S.C., and Jaiswal, J.K. (2014). Imaging Cell Membrane Injury and Subcellular Processes Involved in Repair. J Vis Exp, 51106. 10.3791/51106.
38. Rosa, J.B., Nassman, K.Y., and Sagasti, A. (2022). Sensory axons induce epithelial lipid microdomain remodeling and determine the distribution of junctions in the epidermis. Mol Biol Cell. 10.1091/MBC.E22-09-0396/ASSET/IMAGES/LARGE/MBC-34-AR5-G008.JPEG.
39. O'brien, G.S., Rieger, S., Wang, F., Smolen, G.A., Gonzalez, R.E., Buchanan, J., and Sagasti, A. (2012). Coordinate Development of Skin Cells and Cutaneous Sensory Axons in Zebrafish. J. Comp. Neurol *520*, 816–831. 10.1002/cne.22791.
40. Lee, R.T.H., Asharani, P. v., and Carney, T.J. (2014). Basal Keratinocytes Contribute to All Strata of the Adult Zebrafish Epidermis. PLoS One *9*, e84858. 10.1371/JOURNAL.PONE.0084858.
41. Park, S., Gonzalez, D.G., Guirao, B., Boucher, J.D., Cockburn, K., Marsh, E.D., Mesa, K.R., Brown, S., Rompolas, P., Haberman, A.M., et al. (2017). Tissue-scale coordination of cellular behaviour promotes epidermal wound repair in live mice. Nature Cell Biology 2017 19:3 *19*, 155–163. 10.1038/ncb3472.
42. Kennard, A.S., and Theriot, J.A. (2020). Osmolarity-independent electrical cues guide rapid response to injury in zebrafish epidermis. Elife *9*, 1–27. 10.7554/eLife.62386.
43. Shen, K., Jiang, N., Rasmussen, J.P., Clanton, J.A., Rosenberg, M.F., Luedke, K.P., Cronan, M.R., Parker, E.D., Kim, H.-J., Vaughan, J.C., et al. (2019). A conserved morphogenetic mechanism for epidermal ensheathment of nociceptive sensory neurites. 10.7554/eLife.42455.001.
44. Bonacossa-Pereira, I., Coakley, S., Correspondence, M.A.H., and Hilliard, M.A. (2022). Neuron-epidermal attachment protects hyper-fragile axons from mechanical strain. CellReports *38*, 110501. 10.1016/j.celrep.2022.110501.
45. Gault, W.J., Enyedi, B., and Niethammer, P. (2014). Osmotic surveillance mediates rapid wound closure through nucleotide release. Journal of Cell Biology *207*, 767–782. 10.1083/jcb.201408049.
46. Jelcic, M., Enyedi, B., and Niethammer, P. (2019). Quantitative Imaging of Endogenous and Exogenous H2O2 Gradients in Live Zebrafish Larvae. Methods in Molecular Biology *1982*, 283–299. 10.1007/978-1-4939-9424-3_17.
47. Enyedi, B., and Niethammer, P. (2015). Mechanisms of epithelial wound detection. 10.1016/j.tcb.2015.02.007.
48. Diaz, A.C., Schmidt, N.A., Yamazaki, M., Hsieh, C.J., Lisse, T.S., and Rieger, S. (2022). Coordinated NADPH oxidase/hydrogen peroxide functions regulate cutaneous sensory axon de- and regeneration. Proc Natl Acad Sci U S A *119*, e2115009119. 10.1073/PNAS.2115009119/SUPPL_FILE/PNAS.2115009119.SM18.MOV.
49. Korte, B.G., Giese, M.A., Ramakrishnan, G., Ma, S., Bennin, D., Rindy, J., Dewey, C.N., and Huttenlocher, A. (2022). Cell Type-Specific Transcriptome Profiling Reveals a Role for Thioredoxin During Tumor Initiation. Front Immunol *13*. 10.3389/FIMMU.2022.818893.
50. Chang, S.N., Dey, D.K., Oh, S.T., Kong, W.H., Cho, K.H., Al-Olayan, E.M., Hwang, B.S., Kang, S.C., and Park, J.G. (2020). Phorbol 12-Myristate 13-Acetate Induced Toxicity Study and the Role of Tangeretin in Abrogating HIF-1α-NF-κB Crosstalk In Vitro and In Vivo. Int J Mol Sci *21*, 1–22. 10.3390/IJMS21239261.
51. Pedre, B., Barayeu, U., Ezeriņa, D., and Dick, T.P. (2021). The mechanism of action of N-acetylcysteine (NAC): The emerging role of H2S and sulfane sulfur species. Pharmacol Ther *228*. 10.1016/J.PHARMTHERA.2021.107916.
52. Benvenutti, R., Marcon, M., Reis, C.G., Nery, L.R., Miguel, C., Herrmann, A.P., Vianna, M.R.M., and Piato, A. (2018). N-acetylcysteine protects against motor, optomotor and morphological deficits induced by 6-OHDA in zebrafish larvae. PeerJ *2018*. 10.7717/PEERJ.4957/SUPP-1.

53. Yoo, S.K., Freisinger, C.M., LeBert, D.C., and Huttenlocher, A. (2012). Early redox, Src family kinase, and calcium signaling integrate wound responses and tissue regeneration in zebrafish. J. Cell Biol *199*, 225–234. 10.1083/jcb.201203154.
54. Yoo, S.K., Starnes, T.W., Deng, Q., and Huttenlocher, A. (2011). Lyn is a redox sensor that mediates leukocyte wound attraction in vivo. Nature *480*, 109. 10.1038/NATURE10632.
55. Niethammer, P., Grabher, C., Look, A.T., and Mitchison, T.J. (2009). A tissue-scale gradient of hydrogen peroxide mediates rapid wound detection in zebrafish. Nature. 10.1038/nature08119.
56. Kirfel, G., and Herzog, V. (2004). Migration of epidermal keratinocytes: Mechanisms, regulation, and biological significance. Protoplasma *223*, 67–78. 10.1007/S00709-003-0031-5/METRICS.
57. Mayor, R., and Etienne-Manneville, S. (2016). The front and rear of collective cell migration. Nature Reviews Molecular Cell Biology 2016 17:2 *17*, 97–109. 10.1038/nrm.2015.14.
58. Olson, H.M., and Nechiporuk, A. v. (2021). Lamellipodia-like protrusions and focal adhesions contribute to collective cell migration in zebrafish. Dev Biol *469*, 125. 10.1016/J.YDBIO.2020.10.007.
59. Yamaguchi, N., Zhang, Z., Schneider, T., Wang, B., Panozzo, D., and Knaut, H. (2022). Rear traction forces drive adherent tissue migration in vivo. Nat Cell Biol *24*, 194. 10.1038/S41556-022-00844-9.
60. Kennard, A.S., and Theriot, J.A. (2020). Osmolarity-independent electrical cues guide rapid response to injury in zebrafish epidermis. Elife *9*, 1–27. 10.7554/ELIFE.62386.
61. Bera, K., Kiepas, A., Godet, I., Li, Y., Mehta, P., Ifemembi, B., Paul, C.D., Sen, A., Serra, S.A., Stoletov, K., et al. (2022). Extracellular fluid viscosity enhances cell migration and cancer dissemination. Nature 2022 611:7935 *611*, 365–373. 10.1038/s41586-022-05394-6.
62. Han, L., Mao, Z., Wu, J., Zhang, Y., and Gao, C. (2012). Influences of surface chemistry and swelling of salt-treated polyelectrolyte multilayers on migration of smooth muscle cells. J R Soc Interface *9*, 3455–3468. 10.1098/RSIF.2012.0546.
63. Sforna, L., Michelucci, A., Morena, F., Argentati, C., Franciolini, F., Vassalli, M., Martino, S., and Catacuzzeno, L. (2022). Piezo1 controls cell volume and migration by modulating swelling-activated chloride current through Ca2+ influx. J Cell Physiol *237*, 1857–1870. 10.1002/JCP.30656.
64. Sonnemann, K.J., and Bement, W.M. (2011). Wound Repair: Toward Understanding and Integration of Single-Cell and Multicellular Wound Responses. Annu Rev Cell Dev Biol *27*, 237. 10.1146/ANNUREV-CELLBIO-092910-154251.
65. Enyedi, B., Kala, S., Nikolich-Zugich, T., and Niethammer, P. (2013). Tissue damage detection by osmotic surveillance. Nat Cell Biol *15*, 1123–1130. 10.1038/NCB2818.
66. Mendieta-Serrano, M.A., Mendez-Cruz, F.J., Antúnez-Mojica, M., Schnabel, D., Alvarez, L., Cárdenas, L., Lomelí, H., Ruiz-Santiesteban, J.A., and Salas-Vidal, E. (2019). NADPH-Oxidase-derived reactive oxygen species are required for cytoskeletal organization, proper localization of E-cadherin and cell motility during zebrafish epiboly. Free Radic Biol Med *130*, 82–98. 10.1016/J.FREERADBIOMED.2018.10.416.
67. Norbury, W., Herndon, D.N., Tanksley, J., Jeschke, M.G., and Finnerty, C.C. Infection in Burns. 10.1089/sur.2013.134.
68. Burn Triage and Treatment - Thermal Injuries - CHEMM https://chemm.hhs.gov/burns.htm.
69. Evers, L.H., Bhavsar, D., and Mailänder, P. (2010). The biology of burn injury. Exp Dermatol *19*, 777–783. 10.1111/J.1600-0625.2010.01105.X.
70. Chen, Y.L., and Kan, W.M. (2015). Down-regulation of superoxide dismutase 1 by PMA is involved in cell fate determination and mediated via protein kinase D2 in myeloid leukemia cells. Biochimica et Biophysica Acta (BBA) - Molecular Cell Research *1853*, 2662–2675. 10.1016/J.BBAMCR.2015.07.025.
71. Mocelin, R., Herrmann, A.P., Marcon, M., Rambo, C.L., Rohden, A., Bevilaqua, F., de Abreu, M.S., Zanatta, L., Elisabetsky, E., Barcellos, L.J.G., et al. (2015). N-acetylcysteine prevents stress-induced anxiety behavior in zebrafish. Pharmacol Biochem Behav *139*, 121–126. 10.1016/J.PBB.2015.08.006.
72. Karlsson, A., Nixon, J.B., and McPhail, L.C. (2000). Phorbol myristate acetate induces neutrophil NADPH-oxidase activity by two separate signal transduction pathways: dependent or independent of phosphatidylinositol 3-kinase. J Leukoc Biol *67*, 396–404. 10.1002/JLB.67.3.396.

73. Zafarullah, M., Li, W.Q., Sylvester, J., and Ahmad, M. (2003). Review Molecular mechanisms of N-acetylcysteine actions.
74. Houseright, R.A., Miskolci, V., Mulvaney, O., Bortnov, V., Mosher, D.F., Rindy, J., Bennin, D.A., and Huttenlocher, A. (2021). Myeloid-derived growth factor regulates neutrophil motility in interstitial tissue damage. J Cell Biol *220*. 10.1083/JCB.202103054.
75. Lam, P.Y., Mangos, S., Green, J.M., Reiser, J., and Huttenlocher, A. (2015). In Vivo Imaging and Characterization of Actin Microridges. PLoS One *10*. 10.1371/JOURNAL.PONE.0115639.
76. Akerboom, J., Chen, T.W., Wardill, T.J., Tian, L., Marvin, J.S., Mutlu, S., Calderón, N.C., Esposti, F., Borghuis, B.G., Sun, X.R., et al. (2012). Optimization of a GCaMP Calcium Indicator for Neural Activity Imaging. Journal of Neuroscience *32*, 13819–13840. 10.1523/JNEUROSCI.2601-12.2012.
77. Huemer, K., Squirrell, J.M., Swader, R., Lebert, D.C., Huttenlocher, A., and Eliceiri, K.W. zWEDGI: Wounding and Entrapment Device for Imaging Live Zebrafish Larvae. 10.1089/zeb.2016.1323.
78. Schneider, C.A., Rasband, W.S., and Eliceiri, K.W. (2012). NIH Image to ImageJ: 25 years of image analysis 10.1038/nmeth.2089.
79. Maeda, H., Fukuyasu, Y., Yoshida, S., Fukuda, M., Saeki, K., Matsuno, H., Yamauchi, Y., Yoshida, K., Hirata, K., and Miyamoto, K. (2004). Fluorescent probes for hydrogen peroxide based on a non-oxidative mechanism. Angew Chem Int Ed Engl *43*, 2389–2391. 10.1002/ANIE.200452381.
80. Cornell, R.A., and Eisen, J.S. (2002). Delta/Notch signaling promotes formation of zebrafish neural crest by repressing Neurogenin 1 function. Development *129*, 2639–2648. 10.1242/dev.129.11.2639.
81. Aitkin M, Anderson D, Francis B, and Hinde J (1989). Statistical Modelling in GLIM (Oxford University Press).
82. Long, J.S., and Ervin, L.H. (2000). Using Heteroscedasticity Consistent Standard Errors in the Linear Regression Model. Am Stat *54*, 217. 10.2307/2685594.

Supplemental Information

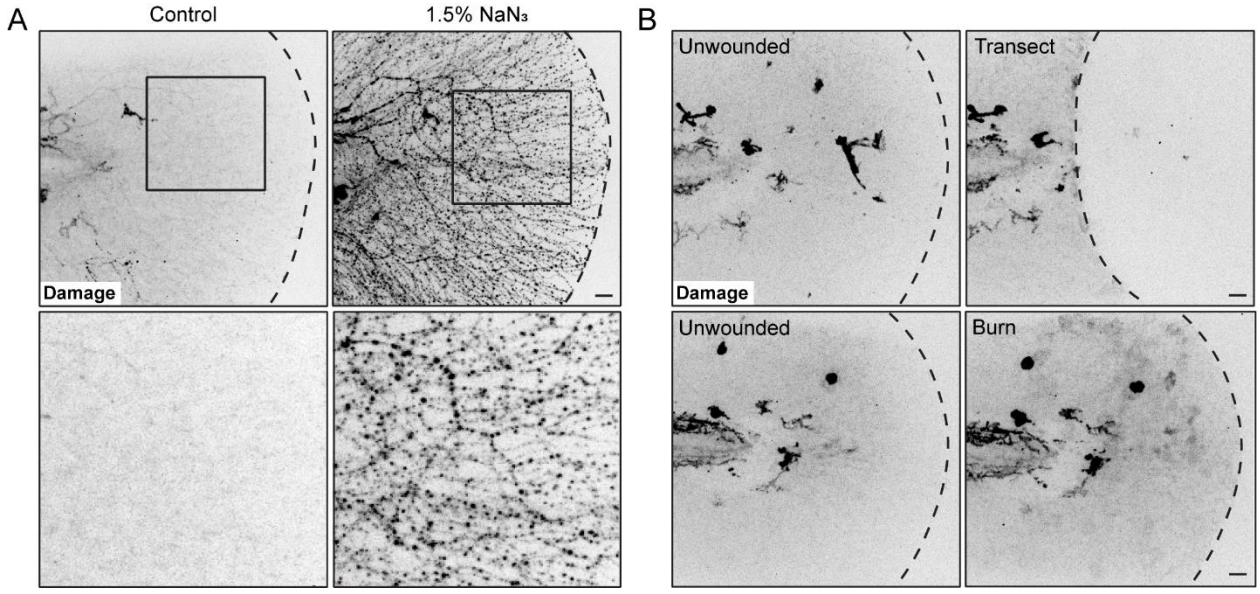

Supplemental Figure 1: Elavl3-GCaMP5 transgenic fish are suitable for visualizing sensory axon damage. (A) Images of neuronal damage in *Tg(Elavl3:GCaMP5)* larval zebrafish caudal fins either untreated or 30 minutes post-treatment with the neurotoxin sodium azide (NaN_3, 1.5% final concentration). Sensory neuron damage is indicated by calcium-positive axon fragments (black dots). Dashed lines denote the fin edge. Black boxes indicated are of inset, shown below. (B) Images of *Tg(Elavl3:GCaMP5)* larvae injected with Ngn1 morpholino before and after the indicated injury. Dashed lines denote the fin edge. In all cases, scale bar=20 µm.

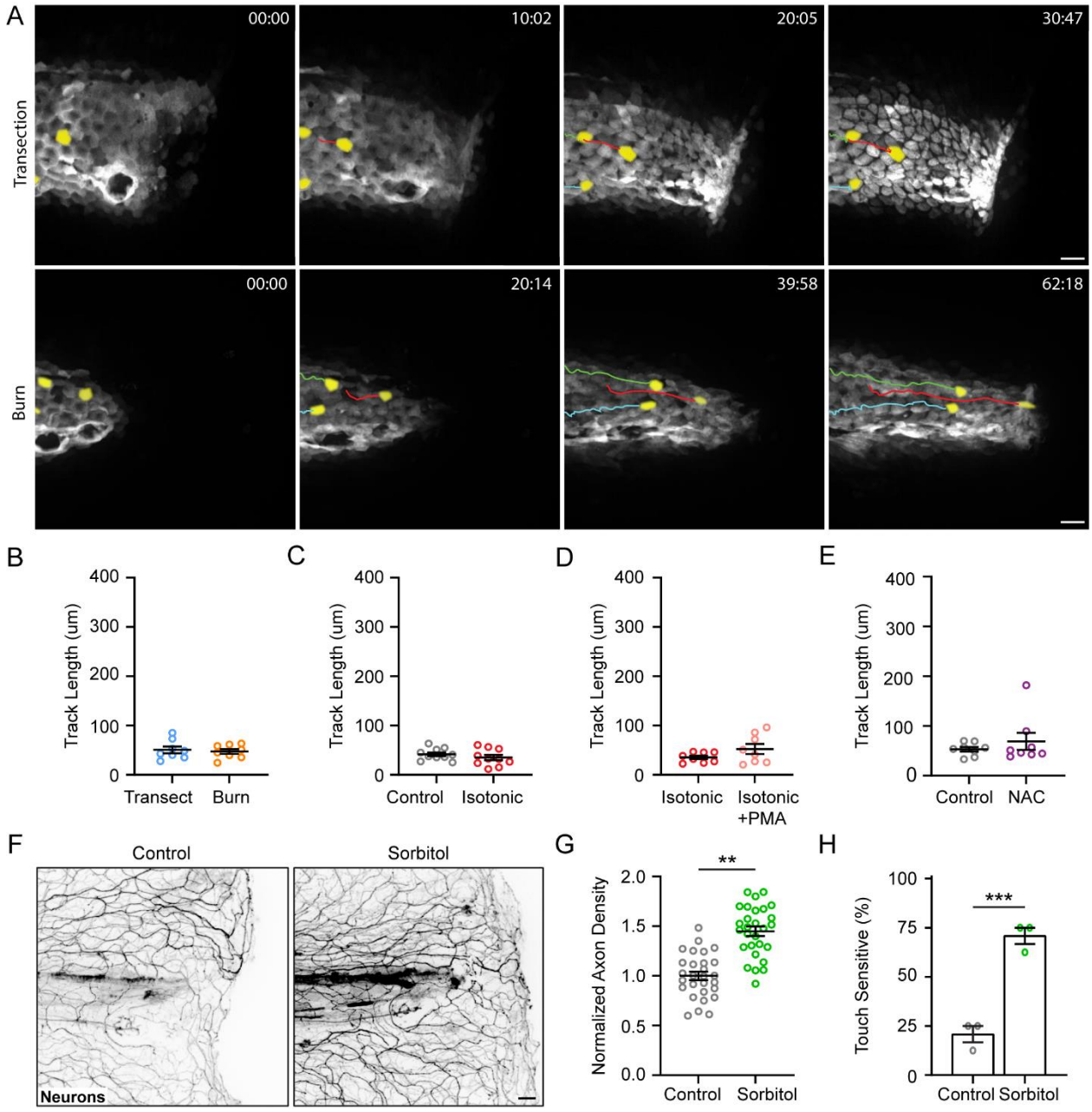

Supplemental Figure 2: Keratinocyte tracking and wounding in the presence of isotonic D-Sorbitol. (A) Time series of basal keratinocyte, *Tg(Krtt1c19e:acGFP)*, movement after the indicated injury. Yellow pseudocolored cells highlight keratinocyte displacement. (B-E) Movement due to fin movement (drift) in cell tracking movies. Plots show fin movement for each larva from experiments shown in Fig. 2E (B, N=8 each), Fig. 3B (C, N=10 each), Fig. 4A (D, N=8 each), and Fig. 4H (E, N=8 each). (F) Representative images of sensory neurons in control and isotonic D-Sorbitol treated larvae 24 hpw. (G) Quantification of axon density in

wounded tissue 24 hpw. N=28 larvae each. (H) Quantification of sensory perception 24 hpw. N=24 larvae each from 3 independent experiments. In all cases, scale bar=20 μm. **p<0.01, ***p<0.001.

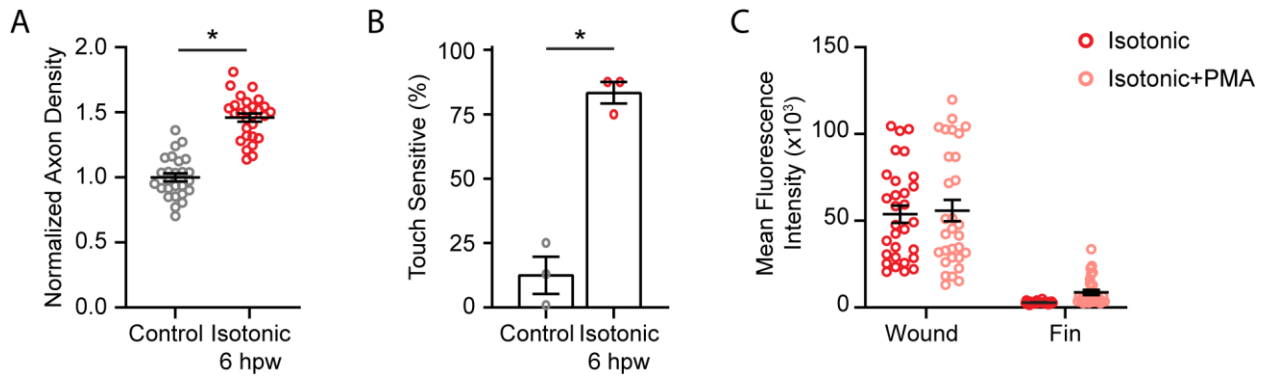

Supplemental Figure 3: Quantification of ROS and axon regeneration in burn-wounded larvae treated with isotonic solution for 6 hours. (A) Quantification of axon density in wounded tissue 24 hpw. N>26 control and 28 treated larvae. (B) Quantification of sensory perception 24 hpw. N=24 larvae each from 3 independent experiments. (C) Quantification of H_2O_2 level (Pfbsf intensity) in larvae treated with isotonic solution with or without PMA for 6 hours. Wound region and fin region are as in Fig. 2E. N=30 larvae each. *p<0.05.

Supplemental Movie Legends

Supplemental Movie 1: Burn injury induces excessive keratinocyte movement. *Tg(Krt4:Utrophin-GFP)* larvae were injured either by tailfin transection (left) or burn (right). While little keratinocyte movement is observed following transection, burn injury results in keratinocyte movement toward the wound edge for approximately 1 hour post-wound. Yellow pseudocolored cells indicate representative keratinocyte movement. Images were collected at 2 frames/min. Scale=20 μm.

Supplemental Movie 2: Epidermal sensory axons move with associated keratinocytes following injury. Basal keratinocyte (magenta), *Tg(Krtt1c19e:Lifeact-Ruby)*, and sensory neuron (cyan), *Tg(Ngn1:GFP-Caax)*, movement was tracked following burn injury. Arrows highlight regions where keratinocyte and sensory axon movement is spatially coincident. Images collected at 3 frames/min. Scale=10 μm.

Supplemental Movie 3: Tissue movement does not induce immediate axonal damage following burn injury. *Tg(Elavl3:GCaMP5)* larva was burn wounded to track axonal damage, indicated by elevated intracellular calcium (black dots). Damage present at time 0 min is due to the burn wound itself, while no additional axonal damage is sustained as a result of tissue movement. Images collected at 2 frames/min. Scale=20 μm.

Supplemental Movie 4: Wounding in isotonic medium prevents burn-induced keratinocyte movement. Basal keratinocyte, *Tg(Krtt1c19e:acGFP)*, movement was tracked in control (left) and isotonic treated (right) larvae following burn injury. Wounding in the presence of isotonic medium prevents keratinocyte movement associated with burn wounding. Yellow pseudocolored cells indicate representative keratinocyte movement. Images were collected at 2 frames/min. Scale=20 μm.